



Interplay of spin–orbit coupling and superconducting correlations in germanium telluride thin films

Vijay Narayan^{*1}, Thuy-Anh Nguyen¹, Rhodri Mansell¹, David Ritchie¹, and Gregor Mussler²

¹ Cavendish Laboratory, Department of Physics, University of Cambridge, J. J. Thomson Avenue, Cambridge CB3 0HE, UK


² Peter Grünberg Institute (PGI-9), Forschungszentrum Jülich, 52425 Jülich, Germany

Received 9 November 2015, revised 1 January 2016, accepted 5 January 2016

Published online 13 January 2016

Keywords GeTe, spin–orbit coupling, superconductivity, weak antilocalization, thin films

* Corresponding author: e-mail vn237@cam.ac.uk

 This is an open access article under the terms of the Creative Commons Attribution License, which permits use, distribution and reproduction in any medium, provided the original work is properly cited.

There is much current interest in combining superconductivity and spin–orbit coupling in order to induce the topological superconductor phase and associated Majorana-like quasiparticles which hold great promise towards fault-tolerant quantum computing. Experimentally these effects have been combined by the proximity-coupling of superconducting leads and high spin–orbit materials such as InSb and InAs, or by controlled Cu-doping of topological insulators such as Bi₂Se₃. However, for practical purposes, a single-phase material which intrinsically displays both these effects is highly desirable. Here we demonstrate coexisting superconducting correlations and spin–orbit coupling in

molecular-beam-epitaxy-grown thin films of GeTe. The former is evidenced by a precipitous low-temperature drop in the electrical resistivity which is quelled by a magnetic field, and the latter manifests as a weak antilocalisation (WAL) cusp in the magnetotransport. Our studies reveal several other intriguing features such as the presence of two-dimensional rather than bulk transport channels below 2 K, possible signatures of topological superconductivity, and unexpected hysteresis in the magnetotransport. Our work demonstrates GeTe to be a potential host of topological SC and Majorana-like excitations, and to be a versatile platform to develop quantum information device architectures.

1 Introduction The confluence of superconductivity and spin–orbit (SO) interactions in the solid-state has presented several opportunities towards fault-tolerant quantum information processing. The SO interaction, born out of the relativistic interplay between the spin and orbital degrees of motion of electrons, manifests as an effective, local magnetic field in the electron's frame of reference. Therefore, when coupled to superconductivity one can expect novel and unconventional pairings [1–3] and, under specific conditions, even emergent 'Majorana'-like quasiparticles [4, 5]. Majorana fermions can have highly non-trivial non-abelian exchange statistics [6] which render them prime candidates for the realisation of qubits, the basic building blocks of a quantum computer. Currently, therefore, there is a large experimental effort towards linking superconductivity and SO interaction through proximity effects [7–14] or by means of delicate intercalated dopants [15, 16]. Here we demonstrate that both these effects coexist

naturally in GeTe, making it a fertile grounds to explore and exploit the interchange between superconductivity and SO interaction without complex materials design and/or device structuring. In particular, we show that the low-temperature (low-*T*) transport characteristics of GeTe reveal both a precipitous drop in resistivity, indicating the onset of superconductivity, as well as unambiguous weak anti-localisation (WAL) signatures due to the strong SO field. Intriguingly, the latter reveal the existence of two-dimensional (2D) conducting states in the bulk films. Finally, we identify several anomalous characteristics in the quantum magnetotransport which can be directly related to the proximity of the superconducting transition. Our results show the single-phase GeTe to be a versatile and convenient platform for applications in quantum information.

In general, the SO field induces a spin-based splitting of energy levels, rendering one spin species more energetically favourable than the other. This would then suggest

the SO interaction to be detrimental to conventional superconductivity which is mediated by Cooper pairs formed from electrons with equal and opposite momenta, and opposite spins. Conversely, however, this might promote the more unconventional, triplet-paired superconductivity. Indeed, the physics underlying superconductors without inversion symmetry, or noncentrosymmetric superconductors, is very rich, defying the very notion of a symmetry-based classification of the superconducting order parameter [1]. Fundamentally, this is because momentum reversal is not a symmetry operation and therefore the various (e.g., s-wave, p-wave, d-wave) symmetries appear mixed. Intriguingly, depending on the relative amplitudes of the s-wave and p-wave components of the superconducting order parameter, it has been shown that there is a transition to a topologically non-trivial state with surface bound states and Majorana zero-modes [17–19]. Equally noteworthy is the unorthodox response of SO coupled superconductors to an in-plane magnetic field wherein the superconductivity is often enhanced rather than destroyed. This has been observed in systems as diverse as films [20] and alloys [21] of Au–Ge, in nanowires of Pb [22], MoGe and Nb [23], Bi thin films [24], Pb thin films [25] and even the conducting electron gas at the interface between LaAlO₃ and SrTiO₃ [25]. In this respect, therefore, GeTe is particularly multifaceted because not only is it inherently superconducting with a strong SO coupling, the SO coupling is intimately linked to the ferroelectric polarisation that spontaneously develops below ≈700 K [26]. The ferroelectric polarisation, in turn, is tunable via an external electric field and enables the reversible switching of the SO field [27].

2 Experimental section

2.1 MBE growth GeTe films were grown by MBE on Si(111) wafers. Prior to the deposition, the Si substrates were chemically cleaned by the HF-last RCA procedure to remove the native oxide and passivate the surface with hydrogen. The substrates were subsequently heated in-situ to 750 °C for 20 min to desorb the hydrogen atoms from the surface. The Ge and Te material fluxes were generated by effusion cells with temperatures of 1250 °C (Ge) and 330 °C (Te). For all samples the Te shutter was opened 2 seconds before the Ge shutter in order to saturate the Si substrate surface with Te. Throughout the growth, the substrate temperature was set at 300 °C. A low growth rate of 5–10 nm hr⁻¹ was chosen in order to obtain a smooth and uniform sample surface. The samples reported in this manuscript have a thickness $t = 34$ nm.

2.2 Fabrication of Hall bars and electrical measurements Hall bars with dimensions 100 μm × 1050 μm were fabricated using photolithography and argon ion milling, and Ti/Au ohmic contacts were deposited using a lift-off process. The devices were subsequently packaged and measured in a He-3 cryostat with a base $T = 280$ mK, and equipped with a 10 T superconducting magnet. The resistance was measured in a standard four-terminal setup with

an excitation current $I_{\text{ex}} = 1$ μA at frequency $f = 17$ Hz. No appreciable nonlinearities in the output voltage appeared even when I_{ex} was increased by a factor of 10.

3 Results and discussion The rhombohedrally distorted unit cell of α-GeTe is schematically depicted in Fig. 1a. The right panel depicts the XRD curve of the investigated GeTe sample. Besides the Si(111) substrate peaks, four peaks originating from the GeTe film are seen. These peaks refer to planes that are all collinear with the (0001) orientation, evidencing that the GeTe film is of single crystal nature with the c -axis in growth direction. Figure 1c and d show the electrical transport characteristics indicating a p-type metal with a carrier concentration $n_p \approx 5.5 \times 10^{26} \text{ m}^{-3}$. This high carrier concentration arises due to spontaneously formed vacancies which impart a metallic character to the nominally semiconducting GeTe [28, 29]. At low T there is a sharp downturn in the electrical resistivity ρ_{xx} , indicating the onset of superconductivity. From the approximately linear trend in ρ_{xx} vs. T above 3 K (shown as a grey dashed line in Fig. 1d), we estimate the onset temperature of superconducting correlations to be ≈1.5 K. A moderate perpendicular magnetic field $B_{\perp} < 0.5$ T (i.e., along the c -axis) suffices to curb the superconductivity, although at the same magnitude of in-plane magnetic field B_{\parallel} , the superconducting transition is still visible. For the thin film samples employed (thickness $t = 34$ nm), this anisotropy likely arises due to the reduced demagnetising factor in this orientation. Notably, the lattice constant of GeTe along the direction of growth $c \approx 1$ nm, and thus we expect that the films are in the ‘bulk’ limit. This is supported by the fact that the superconducting temperature ($T_c \lesssim 0.2$ K) and critical field ($H_c \lesssim 0.5$ T) are consistent with previous reports [30–32] at similar n_p in thicker (>100 nm) films.

The SO coupling has a very pronounced effect on the low- T quantum magnetotransport of materials. As shown in Fig. 2a, in the presence of a perpendicular magnetic field B_{\perp} , the electrical conductivity $\sigma \equiv \rho^{-1}$ shows a pronounced, cusp-like maximum. This so called weak-antilocalisation (WAL) maximum is characteristic of strongly SO coupled systems and stems ultimately from the wave-like nature of the conducting quasiparticles [33]. The destructive self-interference of the quasiparticles as they traverse time-reversed paths results in an enhanced diffusivity which, in turn, manifests as an enhancement in the conductivity. Interestingly, however, the precise form of the maximum, especially at $T < 2$ K, is not consistent with bulk WAL (Fig. 2a inset) [34], but rather indicates a 2D character. The fits in Fig. 2a are to the Hikami–Larkin–Nagaoka (HLN) formula [33] applicable to 2D WAL states with large SO coupling:

$$\begin{aligned} \Delta\sigma_{xx}^{2D} &\equiv \sigma_{xx}^{2D}(B_{\perp}) - \sigma_{xx}^{2D}(0) \\ &= \alpha \frac{e^2}{2\pi^2\hbar} \left[\ln\left(\frac{\hbar}{4eB_{\perp}\ell_{\phi}^2}\right) - \psi\left(\frac{1}{2} + \frac{\hbar}{4eB_{\perp}\ell_{\phi}^2}\right) \right]. \end{aligned} \quad (1)$$

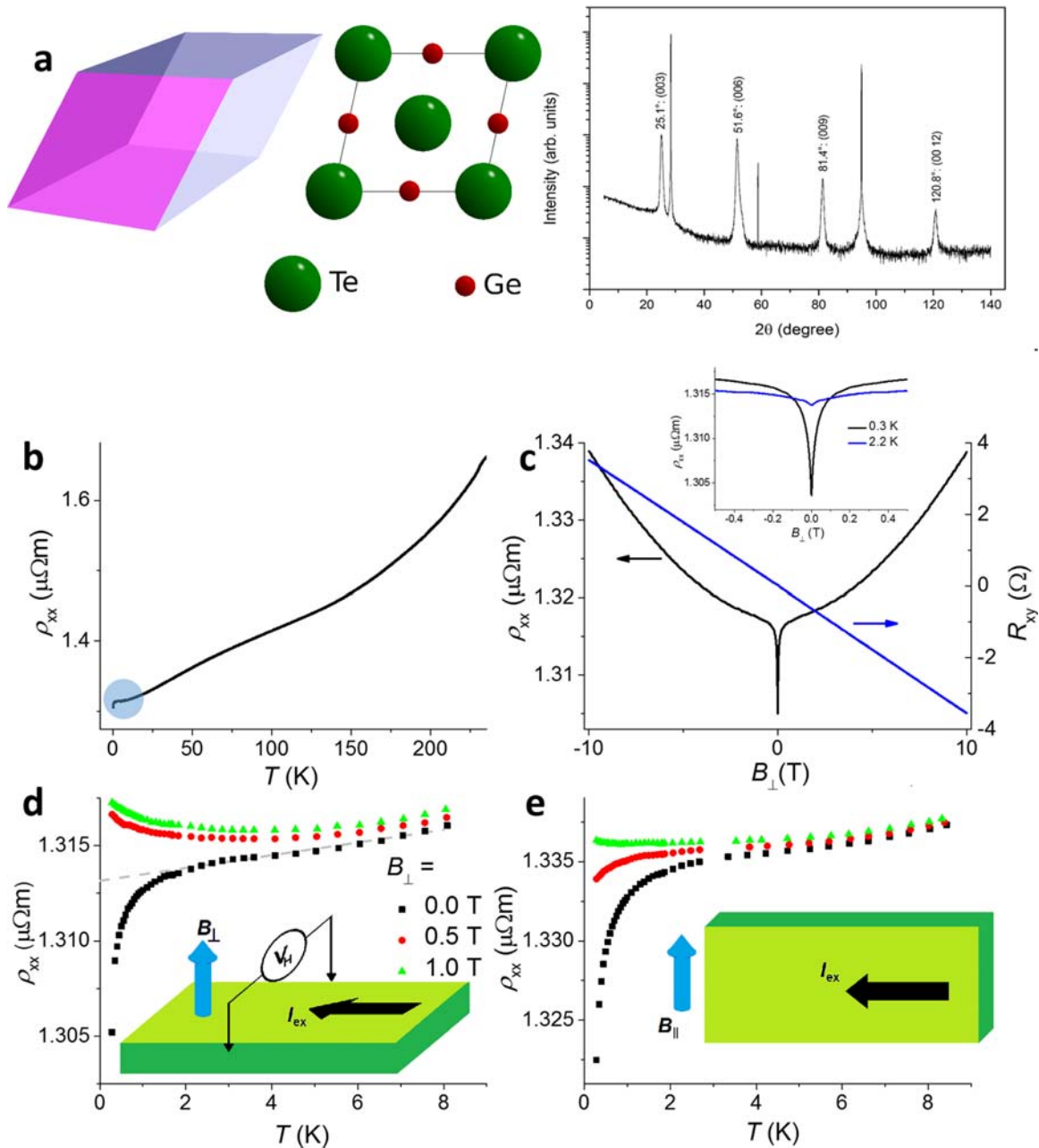


Figure 1 (a) Crystal structure of α -GeTe showing the rhombohedral distortion and lack of inversion symmetry that engenders the strong spin–orbit field. The middle panel shows the arrangement of atoms on the crystal face highlighted in pink. The X-ray diffraction pattern on the right panel reveals a high degree of crystalline order. The unlabeled peaks correspond to the Si(111) substrate. (b)–(e) Electrical transport characteristics. The metal-like increase in ρ_{xx} with T seen in (b) arises due to the large number of spontaneously formed defects [28, 29] for which the Hall resistance R_{xy} in (c) indicates to be p-type. The highlighted region in (b) indicates the superconducting transition which is zoomed into in (d) and (e). As indicated by the dashed grey line in (d), beginning at ≈ 1.5 K there is a steep drop in ρ_{xx} indicating the transition to a superconducting state. The inset in (c) contrasts ρ_{xx} below ($T = 0.3$ K) and above ($T = 2.2$ K) the onset of superconducting correlations. The blue arrows in the insets to (d) and (e) indicate the direction of magnetic field with respect to the sample plane. The critical field H_c at which the superconductivity is destroyed is orientation-dependent, with the in-plane H_c being > 0.5 T.

Here α gets a contribution of 0.5 from each 2D channel, e is the electronic charge, \hbar is Planck’s constant divided by 2π , and ℓ_ϕ is the phase coherence length. For the fits shown in Fig. 2a α and ℓ_ϕ are used as fitting parameters and their

T -dependence is shown in Fig. 2b and c. Equation (1) is seen to describe the data significantly better than a square-root, bulk-like [34] dependence (see Fig. S1, Supporting Information). Indeed, this is consistent with previous an-

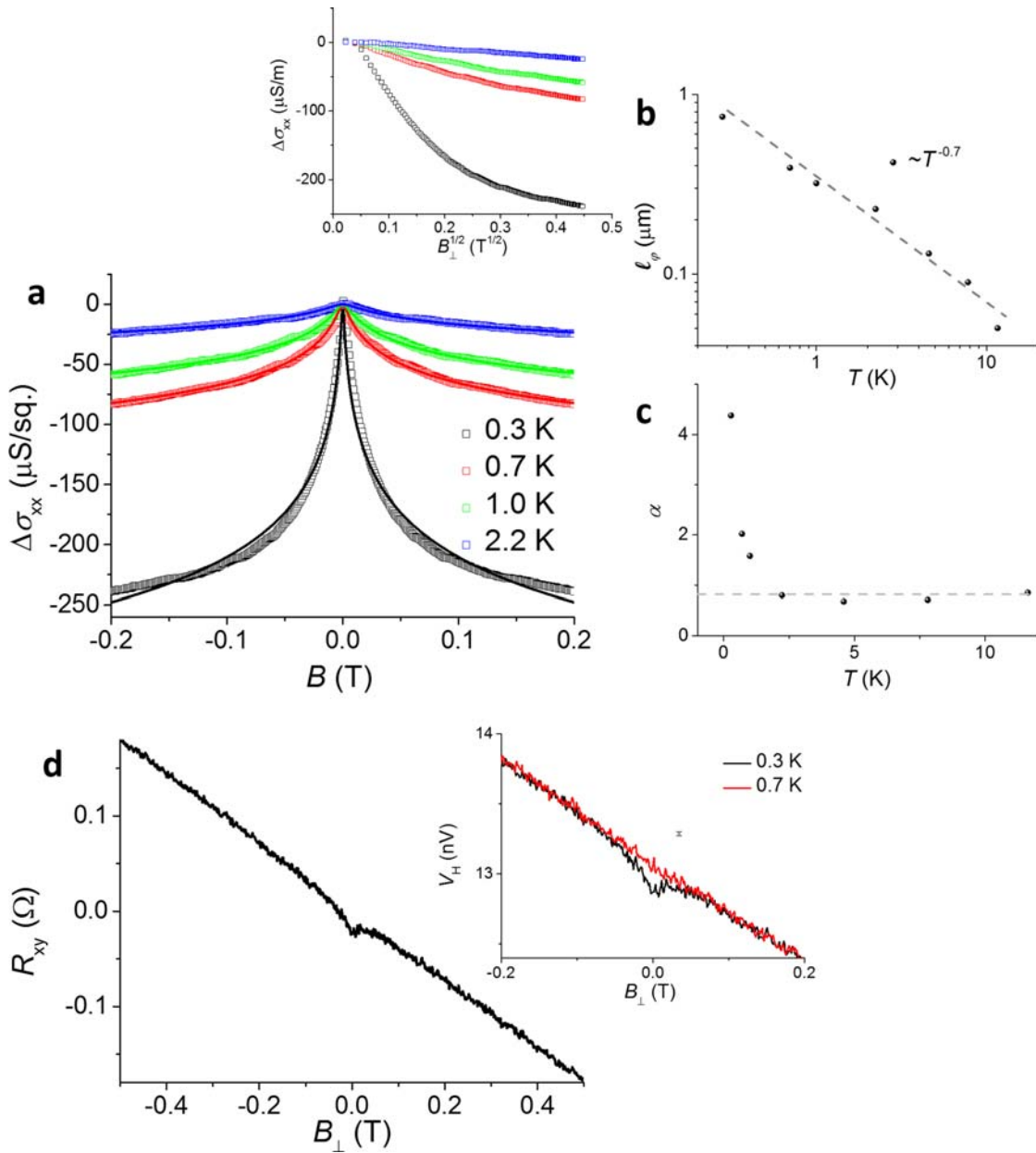


Figure 2 (a) WAL characteristics and corresponding fits to the 2D HLN equation (Eq. (1)). The inset shows that the conductivity corrections, especially between 0.28 K and 1 K, do not scale with $\sqrt{B_{\perp}}$, although at 2 K and above (see Fig. S1 of the Supporting Information), the fits alone do not suffice to discriminate between 2D and bulk behaviour. (b) The phase-coherence length ℓ_{ϕ} decays as $T^{-0.7}$ and (c) α which reflects the number of conducting 2D channels, steeply increases with lowering T . This is likely a consequence of the increased conductivity as the superconducting transition is approached. (d) The superconducting transition also affects the Hall signal with R_{xy} , showing perceptible departure from linearity at small values of $|B_{\perp}|$. As seen from the inset, this is not observed at 0.7 K and above. Also shown is an error bar showing the standard measurement error.

gle-resolved photoemission spectroscopy (ARPES) measurements [35], in which 2D surface states have been evidenced. It is observed that ℓ_{ϕ} decays approximately as T^{-p} with $p = 0.7$, which is faster than $p = 0.5$ as expected for 2D Nyquist scattering due to inter-electron interactions [36]. The dependence of α is more interesting: α is approximately constant for $T \gtrsim 2$ K, but then steeply increases close to the superconducting transition. It is note-

worthy that in Fig. 2a, there are systematic deviations in the HLN fit to the $T = 0.3$ K trace which are not perceptible in the higher T traces (see Fig. S1). The discrepancies can be identified with the zero-field enhancement in σ_{xx} which, in turn, result from the imminent superconductivity. This is in accord with a recent study on Al thin films which show sharp deviations from theoretical expectations as the superconducting transition is approached [37]. At this point

we draw attention to the magneto-conductivity data at 2 K and above which, as is shown in Fig. S1, are equally well fitted by the HLN (i.e., 2D) form as well as the bulk square-root form. Thus, it is not clear from our data whether the conducting states are 2D over the entire T range (as is assumed when extracting the fit parameters plotted in Fig. 2b and c), or whether there is a bulk-to-2D crossover at ≈ 2 K. A third possibility is that the data below 2 K are not indicative of 2D states at all, but simply reflect departures from the bulk form due to the presence of superconducting correlations. However, we believe this to be unlikely since the square-root dependence clearly fails even at 1 K (see Fig. S1) when ρ_{xx} has dropped by less than 0.5% of its value at 2 K. By contrast, the 2D HLN fits are near perfect and only at the lowest achievable T are deviations perceptible. In this context we also note that 2D WAL behavior has been suggested in bulk single crystals of LuPdBi above the superconducting transition [38].

Intriguingly, the superconductivity also appears to leave an imprint on the Hall resistance $R_{xy} \equiv V_H/I_{ex}$ where V_H is the Hall voltage and I_{ex} is the measurement current (see Fig. 1d). It is observed that R_{xy} , while maintaining an overall negative linear slope, displays a dip around $B_{\perp} = 0$ T. We emphasise that the traces have been obtained by averaging several sweeps and that the zero-field feature is well within the limits of experimental resolution. Furthermore, as shown in the inset, this dip is seen only at the lowest T , i.e., closest to the superconducting transition. We note that V_H is not exactly 0 V at $B_{\perp} = 0$ T, but has a small offset ≈ 13 nV that can arise due to minor asymmetries in the relative location of the transverse voltage probes. Thus both the longitudinal (Fig. 1d and e) and Hall voltage

(Fig. 2d) components bear strong signatures of the impending superconductivity.

The data in Fig. 2 suggest that the magnetoresistance in response to B_{\perp} arises largely due to 2D states. In order to probe the bulk properties, therefore, it is necessary to monitor the response to an in-plane field B_{\parallel} . Figure 3a shows several back-and-forth sweeps of ρ_{xx} vs. B_{\parallel} at $T = 0.3$ K. While there is a clear zero-field minimum, the dependence is strongly at odds with WAL: (i) The minimum is significantly broader than the typically expected ~ 100 mT in WAL (see Fig. 2a); (ii) ρ_{xx} is not seen to scale as $\sqrt{|B_{\parallel}|}$; and perhaps most strikingly (iii) there a pronounced hysteresis in the signal. The hysteresis is found to be independent of the rate at which the field is swept (see Fig. S2 of the Supporting Information) and, in fact, the individual down-sweep and up-sweep traces are not even symmetric about their respective minima (see Fig. S2). Furthermore, the hysteresis disappears by $T = 0.7$ K (see inset). These unambiguously show the hysteretic behaviour to be intrinsic to the system and not due to, say, field offsets induced by the magnet power supply. As reported in Fig. 1e, $H_c > 0.5$ T in the parallel orientation and thus, in the following, we consider whether the hysteresis and superconductivity are linked. We first draw attention to the fact that the minimum in ρ_{xx} is sweep direction-dependent. More specifically, when B_{\parallel} is swept from negative to positive (positive to negative) the minimum occurs at a negative (positive) value of field, i.e., there is an offset in the field which reduces the effective magnitude of the field. Since the offset is not sweep-rate-dependent (see Fig. S2) this might be related to the diamagnetism associated with superconductivity. In Fig. 3b we reinspect the perpendicular field magne-

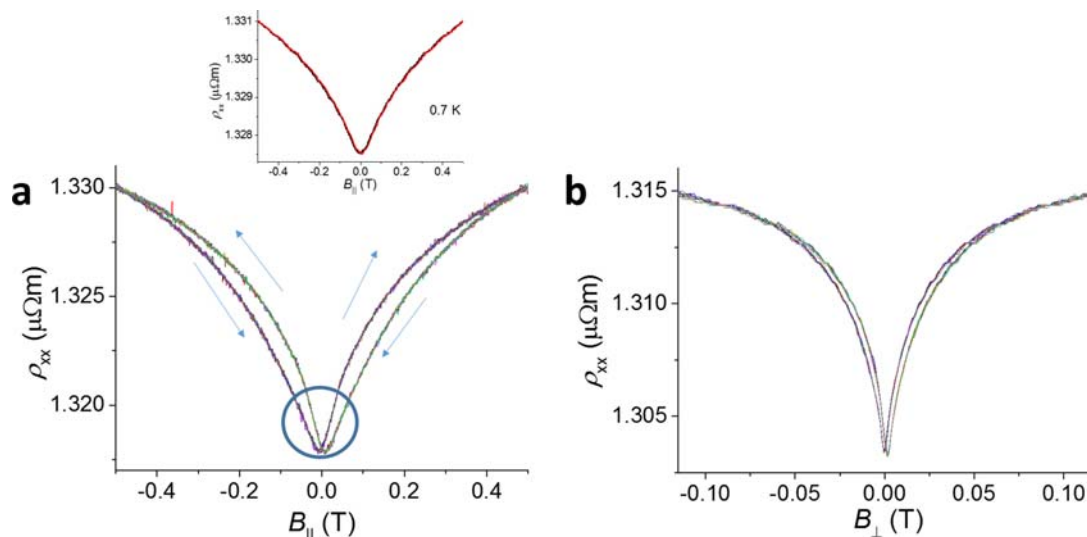


Figure 3 (a) Ten consecutive back-and-forth B_{\parallel} -sweeps showing a strongly hysteretic behaviour. The arrows indicate the sweep direction. Not only is the minimum in ρ_{xx} shifted away from zero, the very shape of the trace appears mirrored in upsweeps and backsweeps. In addition there is a small field negative magnetoresistance. The hysteresis disappears at higher T , although the broad minimum in ρ_{xx} persists. (b) In fact, when several back and forth perpendicular field sweeps are compared one observes a small but definite hysteresis. Notably, the field range over which the hysteresis is observed is smaller, but compares well with the range over which the anomalous dip in V_H is observed. Weak Shubnikov–de Haas-like modulations are observable over and above the WAL lineshape.

toresistance and find that there does indeed seem to be some hysteresis in the signal which is limited to $|B_{\perp}| < 0.1$ T. This field-range is consistent with H_c in the perpendicular orientation in that it coincides remarkably with the range across which the dip in V_H is observed. And finally, the small-field positive magnetoconductivity has been reported in a variety of SO-coupled superconductors [20–25] and even predicted in mesoscopic Ginzburg–Landau superconductors [39]. Thus, in conjunction with the fact that the hysteresis vanishes at the same temperature as do the deviations in the HLN fitting and the ‘dip’ in R_{xy} , the data make a plausible case for the hysteresis to be associated with superconductivity. However, this is admittedly speculative at this stage and, we note that magnetic hysteresis has also been reported in the topological Kondo insulator SmB_6 [40].

In conclusion we present clear evidence that GeTe is an intrinsic SO coupled superconductor. Remarkably, the superconductivity strongly imprints itself in the electrical transport even before the transition occurs, with signatures in the longitudinal and Hall components. The SO coupling manifests clearly in the low-field magnetotransport, but suggests the role of 2D conducting channels. We note that such 2D channels in noncentrosymmetric superconductors can acquire non-trivial topological properties [17–19] which could link some of our intriguing experimental observations to existing work on topological Kondo insulators [40]. While GeTe has received much recent interest due to its multifunctional nature [25, 41–45] the superconducting properties of GeTe and, in particular, their implications in topological technologies have received significantly less attention. Our studies bring these extraordinary properties to the fore and suggest GeTe to be an extremely promising platform for the next generation of quantum technologies.

Supporting Information Supporting Information is available from the Wiley Online Library or from the author.

Acknowledgements V.N., T.-A.N, and R.M. acknowledge funding from EPSRC (UK) and the Leverhulme Trust, UK. G.M. acknowledges financial support from the DFG-funded priority programme SPP1666. V.N. acknowledges useful discussions with Niladri Banerjee, David English, and Edmund Owen. Supporting data for this paper is also available at the DSpace@Cambridge data repository (<https://www.repository.cam.ac.uk/handle/1810/253192>).

References

- [1] L. P. Gorkov and E. I. Rashba, *Phys. Rev. Lett.* **87**, 037004 (2001).
- [2] V. Mineev et al., in: *Non-Centrosymmetric Superconductors: Introduction and Overview*, edited by E. Bauer and M. Sigrist (Springer, 2012).
- [3] S. K Yip, *Annu. Rev. Condens. Matter. Phys.* **5**, 15 (2013).
- [4] R. M. Lutchyn, J. D. Sau, and S. Das Sarma, *Phys. Rev. Lett.* **105**, 077001 (2010).
- [5] Y. Oreg, G. Refael, and F. von Oppen, *Phys. Rev. Lett.* **105**, 077002 (2010).
- [6] F. Wilczek, *Nature Phys.* **5**, 614 (2009).
- [7] M.-X. Wang, C. Liu, J.-P. Xu, F. Yang, L. Miao, M.-Y. Yao, C. L. Gao, C. Shen, X. Ma, X. Chen, Z.-A. Xu, Y. L., S.-C. Zhang, D. Qian, J.-F. Jia, and Q.-K. Xue, *Science* **336**, 52 (2012).
- [8] V. Mourik, K. Zuo, S. M. Frolov, S. R. Plissard, E. P. A. M. Bakkers, and L. P. Kouwenhoven, *Science* **336**, 1003 (2012).
- [9] A. Das, Y. Ronen, Y. Most, Y. Oreg, M. Heiblum, and H. Shtrikman, *Nature Phys.* **8**, 887 (2012).
- [10] M. T. Deng, C. L. Yu, G. Y. Huang, M. Larsson, P. Caro, and H. Q. Xu, *Nano. Lett.* **12**, 6414 (2012).
- [11] A. D. K. Finck, D. J. Van Harlingen, P. K. Mohseni, K. Jung, and X. Li, *Phys. Rev. Lett.* **110**, 126406 (2013).
- [12] S. Nadj-Perge, I. K. Drozdov, J. Li, H. Chen, S. Jeon, J. Seo, A. H. MacDonald, B. A. Bernevig, and A. Yazdani, *Science* **346**, 209 (2014).
- [13] S.-Y. Xu, N. Alidoust, I. Belopolski, A. Richardella, C. Liu, M. Neupane, G. Bian, S.-H. Huang, R. Sankar, C. Fang, B. Dellabetta, W. Dai, Q. Li, M. J. Gilbert, F. Chou, N. Samarth, and M. Zahid Hasan, *Nature Phys.* **10**, 943 (2014).
- [14] J.-P. Xu, C. Liu, M.-X. Wang, J. Ge, Z.-L. Liu, X. Yang, Y. Chen, Y. Liu, Z.-A. Xu, C.-L. Gao, D. Qian, F.-C. Zhang, and J.-F. Jia, *Phys. Rev. Lett.* **112**, 217001 (2014).
- [15] Y. S. Hor, A. J. Williams, J. G. Checkelsky, P. Roushan, J. Seo, Q. Xu, H. W. Zandbergen, A. Yazdani, N. P. Ong, and R. J. Cava, *Phys. Rev. Lett.* **104**, 057001 (2010).
- [16] L. A. Wray, S.-Y. Xu, Y. Xia, D. Hsieh, A. V. Fedorov, Y. S. Hor, R. J. Cava, A. Bansil, H. Lin, and M. Z. Hasan, *Nature Phys.* **7**, 32 (2011).
- [17] A. B. Vorontsov, I. Vekhter, and M. Eschrig, *Phys. Rev. Lett.* **101**, 127003 (2008).
- [18] Y. Tanaka, T. Yokoyama, A. V. Balatsky, and N. Nagaosa, *Phys. Rev. B (R)* **79**, 060505 (2009).
- [19] M. Sato and S. Fujimoto, *Phys. Rev. B* **79**, 094504 (2009).
- [20] Y. Seguchi, T. Tsuboi, and T. Suzuki, *J. Phys. Soc. Jpn.* **61**, 2469 (1992).
- [21] Y. Seguchi, T. Tsuboi, and T. Suzuki, *J. Phys. Soc. Jpn.* **62**, 2564 (1993).
- [22] P. Xiong, A. V. Herzog, and R. C. Dynes, *Phys. Rev. Lett.* **78**, 927 (1997).
- [23] A. Rogachev, T.-C. Wei, D. Pekker, A. T. Bollinger, P. M. Goldbart, and A. Bezryadin, *Phys. Rev. Lett.* **97**, 137001 (2006).
- [24] K. A. Parendo, L. M. Hernandez, A. Bhattacharya, and A. M. Goldman, *Phys. Rev. B* **70**, 212510 (2004).
- [25] H. J. Gardner, A. Kumar, L. Yu, P. Xiong, M. P. Warusawithana, L. Wang, O. Vafek, and D. G. Schlom, *Nature Phys.* **7**, 895 (2011).
- [26] T. Chattopadhyay, J. X. Boucherle, and H. G. von Schnering, *J. Phys. C* **20**, 1431 (1987).
- [27] D. D. Sante, P. Barone, R. Bertacco, and S. Picozzi, *Adv. Mater.* **25**, 3625 (2013).
- [28] A. H. Edwards, A. C. Pineda, P. A. Schultz, M. G. Martin, A. P. Thompson, and H. P. Hjalmarson, *J. Phys.: Condens. Matter* **17**, L329 (2005).
- [29] A. H. Edwards, A. C. Pineda, P. A. Schultz, M. G. Martin, A. P. Thompson, H. P. Hjalmarson, and C. J. Umrigar, *Phys. Rev. B* **73**, 045210 (2006).

- [30] R. A. Hein, J. W. Gibson, R. Mazelsky, R. C. Miller, and J. K. Hulm, *Phys. Rev. Lett.* **12**, 320 (1964).
- [31] P. B. Allen and M. L. Cohen, *Phys. Rev.* **177**, 704 (1969).
- [32] J. L. Smith and P. J. Stiles, *J. Low Temp. Phys.* **26**, 101 (1977).
- [33] S. Hikami, A. I. Larkin, and Y. Nagaoka, *Prog. Theor. Phys.* **63**, 707 (1980).
- [34] A. Kawabata, *Journ. Phys. Soc. Jpn.* **49**, 628 (1980).
- [35] C. Rinaldi, D. Di Sante, A. Giussani, R.-N. Wang, S. Bertoli, M. Cantoni, L. Baldrati, I. Vobornik, G. Panaccione, R. Carlarco, S. Picozzi, and R. Bertacco, <http://arxiv.org/abs/1412.2386> (2014).
- [36] B. Altshuler, V. Tagliacozzo, and A. Tognetti, *Quantum Phenomena in Mesoscopic Systems* (IOS Press, 2003).
- [37] S.-T. Lo, S.-W. Lin, Y.-T. Wang, S.-D. Lin, C.-T. Liang, *Sci. Rep.* **4**, 5438 (2014).
- [38] G. Xu, W. Wang, X. Zhang, Y. Du, E. Liu, S. Wang, G. Wu, Z. Liu, and X. X. Zhang, *Sci. Rep.* **4**, 5709 (2014).
- [39] D. Y. Vodolazov, *Phys. Rev. B* **88**, 014525 (2013).
- [40] S. Wolgast, Y. S. Eo, T. Öztürk, G. Li, Z. Xiang, C. Tinsman, T. Asaba, B. Lawson, F. Yu, J. W. Allen, K. Sun, L. Li, . Kurdak, D.-J. Kim, and Z. Fisk, *Phys. Rev. B* **92**, 115110 (2015).
- [41] M. Chen, K. A. Rubin, and R. W. Barton, *Appl. Phys. Lett.* **49**, 502 (1986).
- [42] B. Sa, J. Zhou, Z. Sun, J. Tominga, and R. Ahuja, *Phys. Rev. Lett.* **109**, 096802 (2012).
- [43] S. Sueya and T. Shintani, *J. Appl. Phys.* **112**, 034301 (2012).
- [44] J. Tominaga, A. V. Kolobov, P. Fons, T. Nakano, and S. Murakami, *Adv. Mater. Interf.* **1**, 1300027 (2013).
- [45] J. Kim, K.-S. Kim, and S.-H. Jhi, *Phys. Rev. Lett.* **109**, 146601 (2012).